Ann. Zool. Fennici 51: 227–244 ISSN 0003-455X (print), ISSN 1797-2450 (online)
Helsinki 7 April 2014 © Finnish Zoological and Botanical Publishing Board 2014

Here be Dragons: Mesowear and tooth enamel isotopes of the classic Chinese "Hipparion" faunas from Baode, Shanxi Province, China

Jussi T. Eronen[1,*], Anu Kaakinen[1], Li-Ping Liu[2], Benjamin H. Passey[3], Hui Tang[1] & Zhao-Qun Zhang[2]

[1)] *Department of Geosciences and Geography, P.O. Box 64, FI-00014 University of Helsinki, Finland (corresponding author's e-mail: jussi.t.eronen@helsinki.fi)*
[2)] *Institute of Vertebrate Paleontology and Paleoanthropology, Chinese Academy of Science, 100044 Beijing*
[3)] *Johns Hopkins University, Department of Earth and Planetary Sciences, 3400 N Charles St, Baltimore MD 21218, USA*

Received 25 Oct. 2013, final version received 20 Jan. 2014, accepted 20 Jan. 2014

Eronen, J. T., Kaakinen, A, Liu, L. P., Passey, B. H., Tang, H. & Zhang, Z. Q. 2014: Here be Dragons: Mesowear and tooth enamel isotopes of the classic Chinese "Hipparion" faunas from Baode, Shanxi Province, China. — *Ann. Zool. Fennici* 51: 227–244.

In this study, we synthesize available data from isotopes, sedimentology and climate modelling together with an extensive mesowear analysis of North Chinese "Hipparion" faunas of Baode. We build on previous research and enlarge the range of analysed localities. Our results show that climate during accumulation of the older localities (7.5 Ma) was more humid than that of the youngest locality (5.7 Ma), while the intermediate localities (~6.5 Ma) accumulated under variable climatic conditions. Our results generally confirm those of previous studies, but highlight temporal and spatial variation within localities. We suggest that this is caused by variation in monsoon strength as evidenced by various proxy records.

Introduction

We want to honour Mikael Fortelius by presenting a review and a summary of the data gathered during our field seasons in the Baode area and in museum collections in Uppsala, Sweden. Fossil mammals from northern China have been known for more than one hundred years (*see* e.g. Schlosser 1903). Much of the material from the classic localities of the Baode area were collected during the extended field campaigns in the 1920s (e.g. Andersson 1923, Zdansky 1923) and deposited in the collections of Uppsala University in Sweden. Because of this Swedish connection, Björn Kurtén, Mikael Fortelius' supervisor, studied the Chinese fossil mammal collections during his M.Sc. and Ph.D. studies (Kurtén 1952, 1953). Kurtén especially elaborated the initial remark of Schlosser (1903) that the Hipparion faunas were separated into northern and southern components with distinct species.

When in 1952 Kurtén published his work on the Chinese Hipparion faunas, he suggested that they comprise three distinct groups: (1) The "gaudryi" faunas, dominated by lower-crowned taxa such as *Gazella gaudryi*, *Honanotherium*,

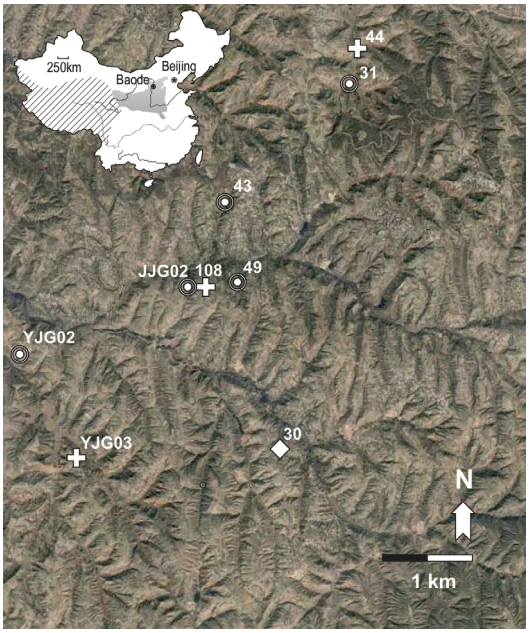

Fig. 1. Map indicating the localities analysed in this study. The small map of China in the upper left corner shows the position of Baode in relation to Loess Plateau (grey shading) and Tibetan Plateau (hatched pattern). The oldest localities are indicated by circles, intermediate localities by crosses, and youngest localities by diamonds.

Dicerorhinus, and cervids, suggesting forest or closed environments, (2) the "dorcadoides" faunas, dominated by higher-crowned taxa such as *G. dorcadoides*, *Chilotherium*, *Samotherium*, *Urmiatherium* and *Plesiaddax*, suggesting a more open steppe environment, and (3) mixed localities that fall somewhere between the two previous faunas. According to Kurtén, the "gaudryi" faunas are situated primarily in the southeast part of the Chinese Loess Plateau, while the "dorcadoides" faunas are primarily in the northwest part of the Loess Plateau. The mixed localities are situated somewhere between these two. Kurtén noted that there are three different possibilities for separation of these faunas (1) temporal separation (2) spatial separation, and (3) both spatial and temporal separation. Kurtén favoured the second, a geographic separation of the localities reflecting environmental zonation, and he regarded all of the Baodean localities as contemporary (e.g. Kurtén 1952, 1985). The idea of two contemporary Hipparion faunas was widely accepted in China until the discovery of two distinct Hipparion faunas in Lantian, Shaanxi Province (Liu *et al.* 1978) where the faunas were found in stratigraphic superposition. This brought into the question the existence of concurrent Hipparion faunas in the Late Miocene of China. Li *et al.* (1984) suggested that Hipparion faunas in China can be divided into two different ages, Bahean and Baodean, correlative to European Vallesian and Turolian stages, respectively, but Qiu and Qiu (1995) did not accepted the Bahean and merged it into Baodean.

When Mikael Fortelius started his work in China in the mid-1990s, the first field campaigns concentrated on the Lantian area, near the city of Xi'an. The stratigraphic work accomplished during the Lantian project established a yardstick for late Miocene Chinese land mammals and showed the Bahe Hipparion fauna to be distinct from and predate the Baode Hipparion faunas (e.g. Zhang *et al.* 2002, 2013b, Kaakinen & Lunkka 2003, Kaakinen 2005). In the early 2000s, the time was mature for returning to the puzzle that was left unsolved by Björn Kurtén, namely the question of spatial-temporal dynamics of the classic Chinese localities of Baode. Following a brief reconnaissance survey in 2001, Fortelius and colleagues mounted a field campaign in 2004 in Baode to investigate the geology and stratigraphy in the area. Using the map published by Zdansky (1923), several of the old Baode localities were relocated in the field and it became possible to place the rich and well-studied Uppsala collection precisely into the composite stratigraphy (*see* Kaakinen *et al.* 2013 for review).

Fossil localities, stratigraphy and depositional environments

Baode is a town in northern Shanxi Province that lies in the northeastern Chinese Loess Plateau west of the Luliang Mountains and east of the Yellow River (Fig. 1). Neogene sediments overlying the Paleozoic basement are grouped into two formations, Baode and Jingle, draped by Quaternary loess-paleosol deposits. Zhu *et al.* (2008) derived a basal age of 7.23 Ma for the

Baode Formation and 5.23 Ma for the boundary between the Baode and Jingle Formations. Both formations are commonly referred to as the late Neogene Red Clay sediments, important deposits of eolian origin underlying the Quaternary loess-paleosol sequence in the Chinese Loess Plateau (e.g. Lu *et al*. 2001, Guo *et al*. 2002). The Pliocene Jingle Formation is composed exclusively of fine grain sizes and its colour is deeper red, while the underlying Baode Formation shows more variable lithologies.

The Baode Formation is conglomeratic towards the base: the basal conglomerate with a clast-supported fabric of subrounded pebbles and cobbles, poorly sorted matrix and relatively high matrix-to-clasts ratio relates to the inception of basin filling in the Baode as recorded also, e.g., in Luzigou (Zhu *et al*. 2008, Pan *et al*. 2011). The remaining sequence consists of red-brown clays and silts punctuated by calcrete horizons that occur at a relatively regular basis every 1–3 meters. This cyclic calcrete occurrence might be indicative of oscillations in the availability of water via groundwater and/or surface runoff. The infrequent sheet conglomerate beds are present throughout the formation but their occurrence does not seem to have a consistent cyclic pattern. The conglomerates are interpreted as being deposited by poorly confined, low-sinuosity, local fluvial systems on the floodplain, sourced from the north and east (Kaakinen *et al*. 2013). Overall, the deposits studied can be regarded as lateral equivalents of the Baode lake sediments which Pan *et al*. (2011) observed in Luzigou, although in our research area true lake facies are not present, and only a few horizons with parallel laminations resulting from deposition in standing water are observed. A grain size distribution analysis (Sukselainen 2008) reveals that an eolian mode of deposition dominates over fluvial during most of the Baode Formation time.

All the known fossiliferous sites are from the Baode Formation. During our field research, we were able to find several of Zdansky's localities (Localities 30, 31, 43, 44, 49, 108) and place them in a stratigraphical framework, along with several new fossil mines currently being quarried in the area (e.g. YJG02, YJG03 and JJG02) (*see* Fig. 1). The fossil occurrences are located in three general levels which were dated by paleomagnetic reversal stratigraphy (Kaakinen *et al*. 2013). The oldest fossil level is established in the lower part of the sequence above the thick basal conglomerate with an age of 7 Ma. The intermediate fossil level (6.5 Ma) is established in the middle of the succession while the youngest (5.7 Ma) is placed high in the Baode Formation. Lithological data do not show any distinguishable differences between the levels, apart from the general upward fining in the mean grain sizes.

Recently published papers (e.g. Passey *et al*. 2009, Kaakinen *et al*. 2013) show that the Baode area is situated near the biome boundary between forest and steppe during the Late Miocene (11–5 Ma). Passey *et al*. (2009) described the possible mechanisms of spatial dynamics for the biome boundary, with retreat and advance of steppe following the strength of the East Asian Summer monsoon. Kaakinen *et al*. (2013) showed that the oldest locality (locality 49) is much more humid than the youngest one (locality 30). Here we present the full analysis of the detailed mesowear investigation of the classic Chinese Hipparion localities from the Baode area together with tooth enamel isotope results. We include all of the localities placed in the stratigraphic context (*see* Kaakinen *et al*. 2013) and discuss the mesowear and enamel isotope results in the context of monsoon dynamics and climate modelling (Tang 2013).

Material

Hypsodonty, mesowear, and stable isotopes were studied on specimens from the Lagrelius Collection at the Museum of Evolution in Uppsala, Sweden. Hypsodonty and mesowear scorings were performed on molar teeth of herbivorous fossil mammals by Jussi T. Eronen, Liu Liping, and Mikael Fortelius in spring 2005. Teeth were sampled for stable isotope analysis in June 2005 by Benjamin H. Passey and Jussi T. Eronen.

Methods

The mesowear analysis, mean hypsodonty, as well as other ecometric analyses were performed by Jussi T. Eronen, and the isotope analysis was

performed by Benjamin H. Passey. The mesowear scoring follows the guidelines of Fortelius and Solounias (2000), where the detailed procedure of mesowear scoring is described. In addition to the fossil data, we used the present-day mammal dataset from Fortelius and Solounias (2000) to analyse the dietary preferences of fossil mammals. We used Ward hierarchical clustering (using statistical program JMP 9.0) to obtain the dietary clusters. We performed the clustering using different groupings. High relief and percentage of rounded cusps were the characters/groupings that best differentiate the material. Other cluster analyses we performed with different characters/groupings gave similar results (not shown here). In addition to mesowear analysis, we calculated the mean hypsodonty for each species based on the specimens, as well as locality specific mean ordinated hypsodonty (HYP) from the data provided in the NOW-database (http://www.helsinki.fi/science/now), following the method of Fortelius *et al*. (2002). We also calculated mean estimated precipitation (MAP) based on the methods of Eronen *et al*. (2010) and Liu *et al*. (2012).

The isotope analysis was performed at the University of Utah following the methods outlined in Passey *et al*. (2009). Note that some of the localities have isotope results but no mesowear data, and vice versa, and it often was not feasible to perform both mesowear analysis and stable isotope analysis on the same tooth specimens. Here we concentrate on the mesowear results, and the localities of interest are selected on that basis. Some of the isotope data was previously reported (Passey 2007, Passey *et al*. 2007, Passey *et al*. 2009 and Kaakinen *et al*. 2013). The sedimentological data are from Kaakinen *et al*. 2013, where they are discussed in detail.

Results

The sample sizes for mesowear scoring were in some cases very low (*see* Table 1). Therefore, we aggregated our data to the genus level. We note that the aggregation of species to genera might mask some of the signal, especially for some genera that have much within-genus variation in their ecological preferences. The most prominent genus in this regard is *Gazella*. Even though all our localities are considered "mixed" in the classic analysis of Kurtén (1952), the individual localities were dominated by one species of *Gazella* (*dorcadoides*, *gaudryi*, or *paotehense*), and locality-specific mesowear results, therefore, represent the dominant group. For other genera, the within-genus ecological preferences are much narrower than for *Gazella*.

Even at the genus level, some locality/genus combinations had low sample sizes and should therefore be treated as suggestive. For genera, we had enough material to analyse *Hipparion*, *Gazella*, *Urmiatherium*, *Paleotragus*, *Cervavitus* and *Chilotherium* (for sample sizes, *n*, *see* Table 1, while for the present-day taxa used in the analysis *see* Table 2). Based on mesowear analysis (Fig. 2), Hipparions from locality 30 (n = 17) grouped together with grazers, locality 49 (n = 3) and 43 (n = 12) had more mixed diet than hipparions from locality 30. Hipparions from locality 31 (n = 2) clustered close to brachydont browsers although the sample size was low. Hipparions from locality 44 (n = 6) were grouped together with Indian and Sumatran rhinos suggesting that they are more browse-dominated than hipparions from other localities.

Gazelles from locality 30 (n = 26) grouped close to hipparions from localities 49 and 43, but with more brachydont taxa (mixed feeders; *Capra ibex*, *Giraffa camelopardis*, *Capreolus capreolus*, *Antilocapra americana* and *Antidorcas marsupialis*). Gazelles from localities 108 (n = 2) and 44 (n = 2) grouped together with brachydont browsers. Gazelles from locality 49 (n = 10) were similar to brachydont browsers. *Urmiatherium* from locality 30 (n = 31) grouped with grazers, while *Urmiatherium* from 49 (n = 5) grouped with *Dendrohyrax dorsalis* (a browser) and *Urmiatherium* from locality 108 (n = 2) grouped with brachydont browsers.

Paleotragus from locality 49 (n = 3) grouped with mesodont mixed feeders. *Paleotragus* from locality 43 (n = 3) grouped with brachydont browsers. *Paleotragus* from locality 108 (n = 8) grouped close to serow (mixed hypsodont). *Paleotragus* from locality 30 (n = 2) was grouped with mixed feeders (seasonal diet change). *Cervavitus* from locality 49 (n = 2)

Table 1. The Mesowear scoring data for the Baode region localities; *n* = number of specimens.

Genus-locality	ID	*n*	Mesowear scoring									
			High		Low		Sharp		Rounded		Blunt	
			Number	%	Number	%	Number	%	Number	%	Number	%
Chilotherium-30	YOUNG_Chi-30	6	6	100		0	1	16	5	83		0
Gazella-30	YOUNG_Gaz-30	26	26	100		0	18	69	8	30		0
Hipparion-30	YOUNG_Hip-30	17	11	64	6	35	6	35	11	64		0
Palaeotragus-30	YOUNG_Pal-30	2	2	100		0	1	50	1	50		0
Samotherium-30	YOUNG_Sam-30	17	15	88	2	11	1	5	16	94		0
Sinotragus-30	YOUNG_Sin-30	10	9	90	1	10	7	70	3	30		0
Tragoreas-30	YOUNG_Tra-30	2	2	100		0		0	2	100		0
Urmiatherium-30	YOUNG_Urm-30	31	26	83	5	16	8	25	23	74		0
Chilotherium-31	OLD_Chi-31	3	2	66	1	33		0	3	100		0
Hipparion-31	OLD_Hip-31	2	2	100		0		0	2	100		0
Sinotherium-31	OLD_St-31	2		0	2	100	2	100		0		0
Tragoreas-31	OLD_Tra-31	2	2	100		0	2	100		0		0
Chilotherium-43	OLD_Chi-43	5	4	80	1	20	1	20	4	80		0
Gazella-43	OLD_Gaz-43	3		0	3	100	1	33		0	2	66
Hipparion-43	OLD_Hip-43	12	12	100		0	8	66	4	33		0
Palaeotragus-43	OLD_Pal-43	3	3	100		0		0	3	100		0
Samotherium-43	OLD_Sam-43	2	1	50	1	50		0	2	100		0
Urmiatherium-43	OLD_Urm-43	2	1	50	1	50		0	2	100		0
Cervavitus-44	INTERMEDIATE_Cer-44	5	5	100		0	2	40	3	60		0
Gazella-44	INTERMEDIATE_Gaz-44	2	2	100		0	2	100		0		0
Hipparion-44	INTERMEDIATE_Hip-44	6	6	100		0	5	83	1	16		0
Acerorhinus-49	OLD_Ac-49	2	2	100		0	2	100		0		0
Cervavitus-49	OLD_Cer-49	2	2	100		0	1	50	1	50		0
Gazella-49	OLD_Gaz-49	10	10	100		0	9	90	1	10		0
Honanotherium-49	OLD_Hon-49	2	2	100		0		0	2	100		0
Palaeotragus-49	OLD_Pal-49	3	3	100		0	1	33	2	66		0
Urmiatherium-49	OLD_Urm-49	5	4	80	1	20	2	40	3	60		0
Hipparion-49	OLD_Hip-49	3	3	100		0	2	66	1	33		0
Chilotherium-51	Chi-51	3	3	100		0	1	33	2	66		0
Gazella-52	Gaz-52	4	4	100		0	4	100		0		0
Hipparion-52	Hip-52	3	3	100		0	3	100		0		0
Hipparion-57	Hip-57	2		0	2	100		0		0	2	100

continued

Table 1. Continued.

Genus-locality	ID	*n*	Mesowear scoring									
			High		Low		Sharp		Rounded		Blunt	
			Number	%	Number	%	Number	%	Number	%	Number	%
Cervavitus-58	Cer-58	2	2	100		0		0	2	100		0
Hipparion-70	Hip-70	9	9	100		0	3	33	6	66		0
Cervavitus-71	Cer-71	5	5	100		0	3	60	2	40		0
Cervavitus-73	Cer-73	16	16	100		0	10	62	6	37		0
Gazella-73	Gaz-73	7	7	100		0	2	28	5	71		0
Hipparion-73	Hip-73	5	5	100		0	2	40	3	60		0
Hipparion-77	Hip-77	2	2	100		0	1	50	1	50		0
Cervavitus-78	Cer-78	3	3	100		0	1	33	2	66		0
Gazella-78	Gaz-78	2	2	100		0	2	100		0		0
Eostyloceros blainvillei-81	Eos-81	2	2	100		0		0	2	100		0
Gazella-108	INTERMEDIATE_Gaz-108	2	2	100		0	2	100		0		0
Palaeotragus-108	INTERMEDIATE_Pal-108	8	8	100		0	3	37	5	62		0
Urmiatherium-108	INTERMEDIATE_Urm-108	2	2	100		0		0	2	100		0
Gazella-109	Gaz-109	12	12	100		0	10	83	2	16		0
Palaeotragus-109	Pal-109	3	3	100		0	1	33	2	66		0
Palaeotragus-110	Pal-110	2	2	100		0		0	2	100		0
Tragoreas-110	Tra-110	4	4	100		0	3	75	1	25		0
Gazella-114	Gaz-114	16	15	93	1	6	9	56	6	37	1	6
Hipparion-114	Hip-114	2	2	100		0	1	50	1	50		0
Palaeotragus-114	Pal-114	2	2	100		0	1	50	1	50		0
Plesiaddax-114	Ples-114	10	10	100		0	2	20	8	80		0
Samotherium-115	Sam-115	2	2	100		0	1	50	1	50		0
Gazella-116	Gaz-116	2	2	100		0	1	50	1	50		0
Palaeotragus-116	Pal-116	4	4	100		0	1	25	3	75		0
Samotherium-116	Sam-116	3	3	100		0		0	3	100		0
Cervavitus-Yushe	Cer-Yushe	7	6	85	1	14	4	57	3	42		0

grouped with mesodont mixed feeders (seasonal diet change), while *Cervavitus* from locality 44 (n = 5) grouped with hypsodont mixed feeders/brachydont browsers. *Chilotherium* from locality 43 (n = 5) grouped with hypsodont grazers, while *Chilotherium* from locality 30 (n = 6) grouped with browsers.

In addition to individual genera, we also analysed the mesowear within and between localities. Due to small sample sizes and stratigraphic restrictions (*see* Kaakinen *et al*. 2013), we concentrate here on the following localities that we can reliably place in chronologic order: 30, 31, 43, 44, 49 and 108. Here we used the provisional separation of localities into three groups: Old (7 Ma), Intermediate (6.5 Ma), and Young (5.7 Ma), based on Kaakinen *et al*. (2013). We also provide MAP estimates for each locality based on calculations using the methods of Eronen *et al*. (2010) and Liu *et al*. (2012). The localities between the oldest (49) and youngest (30) represented the most humid and arid climates, respectively (Table 3 and Fig. 2). The oldest locality (49) had the highest precipitation estimate, even among the old localities. The taxa at locality 49 had browser-dominated diets, with some component of mixed feeding, possibly seasonal changes. The other two old localities, 43 and 31, showed similar dietary adaptations among the taxa, but with some possible grazers (e.g. *Chilotherium*), and lower precipitation estimates. The intermediate localities, 108 and 44, had similar estimated precipitation ranges as the old localities (43 and 31), but the taxa present at these localities showed clear dominance

Table 2. The acronyms used in Fig. 2 for present-day species in the mesowear analysis. Based on Fortelius and Solounias 2000. Species names set in all caps = browsers, genus set in all caps species in lower case = mixed-feeders, species names set in lower case = grazers.

Species	ID	Species	ID
DENDROHYRAX ARBOREUS	DA	TRAGELAPHUS angasi	TA
DENDROHYRAX DORSALIS	DD	TRAGELAPHUS imberbis	TI
CEPHALOPHUS DORSALIS	DR	TETRACERUS quadricornis	tq
HETEROHYRAX BRUCEI	HB	BOSELAPHUS tragocamelus	Tr
HYAEMOSCHUS AQUATICUS	HY	TRAGELAPHUS STREPSICEROS	TT
CEPHALOPHUS NATALENSIS	NA	ALCES ALCES	AA
CEPHALOPHUS NIGER	NG	alcelaphus buselaphus	ab
CEPHALOPHUS NIGRIFRONS	NI	bison bison	bb
PROCAVIA capensis	Pc	CARPICORNIS sumatrensis	Ca
CEPHALOPHUS SILVICULTOR	SL	CERVUS canadanensis	Cc
alcelaphus lichtensteinii	al	ceratotherium simum	cs
ANTILOPCAPRA AMERICANA	AM	connochaetes taurinus	ct
AXIS porcinus	ap	DICEROS BIRCORNIS	DB
AXIS axis	ax	damaliscus lunatus	dl
BOOCERCUS EURYCEROS	BE	DICERORHINUS SUMATRENSIS	DS
BUDORCAS taxicolor	BT	equus burchelli	eb
CERVUS duvauceli	cd	equus grevyi	eg
CAPRA ibex	Ci	GIRAFFA CAMELOPARDIS	GC
CAMELUS dromedarius	CL	GAZELLA granti	Gg
CERVUS unicolor	Cu	GAZELLA thomsonii	Gt
AMMODORCAS CLARKEI	EI	hippotragus equinus	he
LAMA glama	Lg	hippotragus niger	hn
LAMA vicugna	Lv	kobus ellipsiprymnus	ke
LITOCRANIUS WALLERI	LW	AEPYCEROS melampus	Me
ANTIDORCAS marsupialis	Ma	ODOCOILEUS HEMIONUS	OH
OVIS canadensis	Oc	OKAPI JOHNSONII	OJ
CAPREOLUS CAPREOLUS	OL	OVIBOS moschatus	Om
OUREBIA ourebi	oo	ODOCOILEUS VIRGIANUS	OV
REDUNCA fulvorufula	rf	redunca redunca	rr
RHINOCEROS unicornis	Ru	RHINOCERUS SONDAICUS	RS
SYNCERUS caffer	sc	TAUROTRAGUS oryx	To
SAIGA tatarica	St	TRAGELAPHUS sciptus	Ts

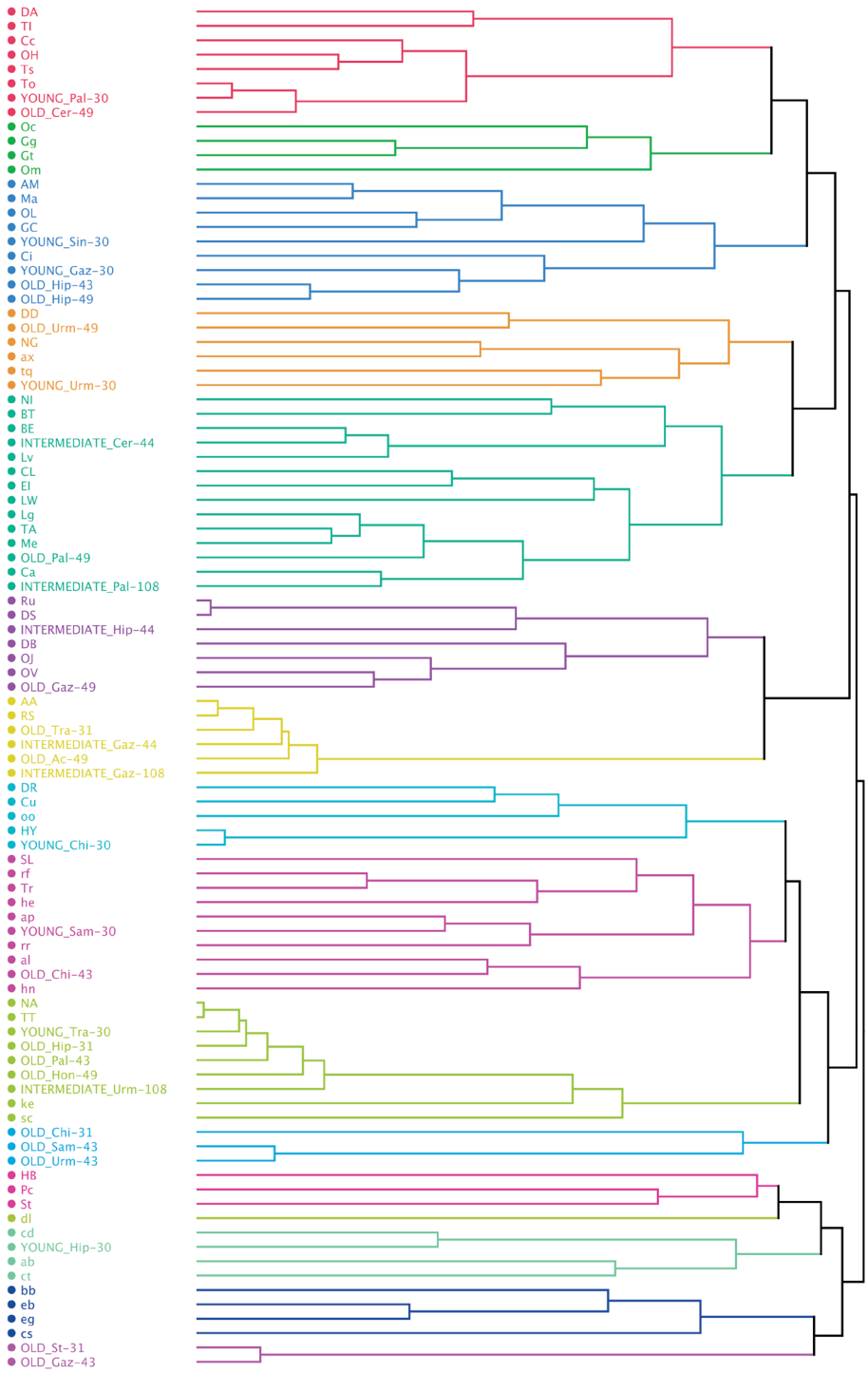

Fig. 2. Mesowear grouping based on hierarchical clustering. The abbreviations used are shown in Table 1 (for fossil taxa) and Table 2 (for extant taxa). For the extant species, capitalized acronym indicates browsers, lower case acronym indicates grazer, and mixed indicates mixed diet. For fossils the acronym indicates temporal sequence (old, intermediate or young locality), locality number and genus acronym. The colours indicate preliminary grouping to similar diets based on mesowear signal.

Table 3. The locality specific environmental data for the analysed localities. In addition to the mean annual precipitation estimates (MAP), we provide also mean hypsodonty score and description of mesowear signal in each locality.

Group	Locality	MAP estimates	Mean HYP	Mesowear description
Old (about 7 Ma)	49	1426 mm (Eronen *et al*. 2010), 748 mm (Liu *et al*. 2012)	1.53	Hipparions group with mixed feeders. *Paleotragus* groups with mesodont mixed feeders. *Cervavitus* groups with mesodont mixed feeders (seasonal diet change). Gazellas group with brachydont browsers. *Acerorhinus* groups with brachydont browsers. *Urmiatherium* groups with brachydont browsers.
Old (about 7 Ma)	43	1405 mm (Eronen *et al*. 2010), 578 mm (Liu *et al*. 2012)	1.81	Hipparions group with mixed feeders, *Chilotherium* groups with hypsodont grazers, *Paleotragus* groups with brachydont browsers
Old (about 7 Ma)	31	681 mm (Eronen *et al*. 2010), 345 mm (Liu *et al*. 2012)	2.09	*Tragoreas* is close to brachydont browsers. *Hipparion* is close to brachydont browsers.
Intermediate (around 6.5 Ma)	108	681 mm (Eronen *et al*. 2010), 297 mm (Liu *et al*. 2012)	1.9	*Paleotragus* groups close to serow (mixed hypsodont). *Gazelle* groups with brachydont browsers. *Urmiatherium* from 108 groups with brachydont browsers.
Intermediate (around 6.5 Ma)	44	1426 mm (Eronen *et al*. 2010), 617 mm (Liu *et al*. 2012)	1.86	*Cervavitus* groups with hypsodont mixed feeder / brachydont browser. *Hipparion* group with rhinos. *Gazellas* group with brachydont browsers
Young (about 5.7 Ma)	30	681 mm (Eronen *et al*. 2010), 317 mm (Liu *et al*. 2012)	2.11	*Chilotherium* groups with browsers. *Tragoreas* groups with browsers. *Gazella dorcadoides* is close to mixed feeder brachydonts, while *G.paothense* is close to brachydont browsers. *Paleotragus* is grouped with mixed feeders (seasonal diet change), *Sinotragus* is close to mesodont browsers. *Samotherium* groups with grazers. Hipparions group with grazers, as well as *Urmiatherium.*

of browsers, with less mixed feeding or grazing taxa. Even hipparions from locality 44 group with Indian and Sumatran rhinos. The young locality (30) had lowest precipitation estimates, and the taxa were more dominated by mixed feeders and even "pure" grazers.

Isotopes

The carbon isotope results (Table 4 and Fig. 3) showed a general correspondence between diet and hypsodonty, with brachydont taxa seldom eating C4 vegetation (except *Paleotragus* at locality 30), and mesodont and hypsodont taxa showing mixed C3/C4 diets (Fig. 3). There was also a general correspondence between stable isotopes and mesowear, with species that are exclusively C3 feeders at all localities having exclusively high cusp relief, and mixed C3/C4 feeders showing variable cusp relief (Fig. 3). The isotope results were resolved at the species level for gazelles. Noteworthy is the slight difference between *G. dorcadoides* and *G. paotehense* at

Table 4. The enamel carbon isotope results from Baode fossils.

Sample ID	Taxon	Locality	Tooth	δ^{13}C (PDB)	%C4
CN2004-BD-16	*Capra* or *Ovis* (domestic)	recent	cheek	–7.9	21
CN2004-BD-164-p3	*Capra* or *Ovis* (domestic)	recent	p3	–10.6	0
CN2004-BD-13-p3	*Sus* (domestic)	recent	p3	–5.6	40
CN2004-BD-163-m1	*Sus* (domestic)	recent	m1	–4.7	48
CN2004-BD-165-M2	*Sus* (domestic)	recent	M2	–5.4	42
M11320	*Gazella* sp. *paotehensis*	30	lm3	–11.8	0
M11344	*Gazella* sp. *paotehensis*	30	rm3	–9.4	0
M11345	*Gazella* sp. *paotehensis*	30	lm3	–8.5	1
M11487	*Gazella* cf. *Dorcadoides*	30	rm3	–8.9	0
M11490	*Gazella* cf. *Dorcadoides*	30	lM3	–7.6	9
M11493	*Gazella* cf. *Dorcadoides*	30	rP4	–7.9	6
M11502	*Gazella* cf. *Dorcadoides*	30	lM3	–6.3	19
M11813	*Tragoreas lagrelii*	30	m3	–7.2	11
M11815	*Tragoreas lagrelii*	30	m3	–8.4	1
M11817	*Tragoreas anderssoni*	30	rm3	–8.5	1
M11822	*Tragoreas anderssoni*	30	rm2	–7.1	12
M11823	*Tragoreas anderssoni*	30	lm3	–7.9	6
M11845	*Tragoreas* sp.	30	lM2	–10.1	0
M10043	*Urmiatherium intermedium*	30	rM3	–8.7	0
M10631	*Urmiatherium intermedium*	30	rM3	–6.6	17
M10633	*Urmiatherium intermedium*	30	rM3	–7.8	7
M10640	*Urmiatherium intermedium*	30	lM3	–5.6	25
M10647	*Urmiatherium intermedium*	30	lM3	–7.4	10
M10648	*Urmiatherium intermedium*	30	rM3	–7.1	12
M9813	Pliocervid	30	rM3	–8.7	0
M9820	Pliocervid	30	lm3	–10.4	0
M9824	Pliocervid	30	rm3	–9.2	0
M9826	Pliocervid	30	rm3	–9.6	0
M9828	Pliocervid	30	rm3	–10.8	0
M268	*Hipparion dermatorhinum*	30	rP2	–8.6	0
M303	*Hipparion fossatum*	30	lM3	–4.6	34
M304	*Hipparion fossatum*	30	lP2	–7.9	6
M3822	*Hipparion fossatum*	30	lm3	–7.8	7
L30 Hipp-1	*Hipparion kreugeri*	30	cheek	–10.1	0
L30 Hipp-5	*Hipparion kreugeri*	30	cheek	–10.3	0
L30 Hipp-6	*Hipparion kreugeri*	30	cheek	–7.5	9
L30Hipp5.p	*Hipparion kreugeri*	30	cheek	–10.2	0
M343	*Hipparion platyodus*	30	lm3	–6.8	15
L30 Hipp-3	*Hipparion ptychodus*	30	cheek	–8.3	2

continued

Table 4. Continued.

Sample ID	Taxon	Locality	Tooth	δ^{13}C (PDB)	%C4
L30 Hipp-2	*Hipparion richthofeni*	30	cheek	–8.7	0
L30 Hipp-4	*Hipparion richthofeni*	30	cheek	–7.4	10
M274	*Hipparion richthofeni*	30	rp2	–7.9	6
M276	*Hipparion richthofeni*	30	lm1	–9.7	0
M7989	*Hipparion richthofeni*	30	lm3	–7.4	10
L30 Paleotragus	*Paleotragus* sp.	30	P3 or P4	–7.7	8
M11014	*Paleotragus microdon*	30	rM3	–6.9	14
M11017-frag	*Paleotragus* sp. *microdon*	30	lm3	–9.0	0
M11017-p	*Paleotragus* sp. *microdon*	30	lm3	–8.8	0
M11033	*Paleotragus microdon*	30	rM3	–8.1	4
M10790	*Samotherium* sp. 1	30	rm3	–7.3	11
M10791	*Samotherium* sp. 1	30	lm3	–7.7	7
M10792	*Samotherium sinense*	30	M1 or M2	–6.6	17
M10793	*Samotherium sinense*	30	M1 or M2	–6.8	15
M10794	*Samotherium* sp. 1	30	rM1	–8.8	0
M1308	*Sinotragus wimani*	30	lM3	–8.2	3
M1828	*Sinotragus wimani*	30	lM3	–8.3	3
M7420	*Chilotherium* sp. cf. *anderssoni*	30	CHEEK	–10.2	0
M7422	*Chilotherium* sp. cf. *anderssoni*	30	CHEEK	–9.1	0
M7423	*Chilotherium* sp. cf. *anderssoni*	30	CHEEK	–10.0	0
M7424	*Chilotherium* sp. cf. *anderssoni*	30	CHEEK	–9.0	0
M7421	*Chilotherium* sp. cf. *anderssoni*	30	CHEEK	–7.4	10
M7422.p	*Chilotherium* sp. cf. *anderssoni*	30	CHEEK	–9.1	0
M11792	*Tragoreas lagrelii*	43	m3	–7.4	10
M11794	*Tragoreas lagrelii*	43	lm3	–8.5	1
M11841	*Tragoreas paleosinensis*	43	lp3	–9.1	0
M11841	*Tragoreas paleosinensis*	43	lp3	–9.7	0
M11793	*Tragoreas lagrelii*	43	lm3	–7.6	8
M10529	*Urmiatherium intermedium*	43	lM3	–5.7	25
M10558	*Urmiatherium intermedium*	43	rm3	–7.9	6
M10570	*Urmiatherium intermedium*	43	rm3	–7.4	10
M10679	*Urmiatherium intermedium*	43	M2	–7.5	9
M248	*Hipparion hippidiodus*	43	lM3	–7.0	13
M249	*Hipparion hippidiodus*	43	CHEEK	–6.8	15
M310	*Hipparion coelophyes*	43	lP4	–9.6	0
M3823	*Hipparion dermatorhinum*	43	lM3	–5.1	29
M251	*Hipparion hippidiodus*	43	CHEEK	–9.3	0
M7527	*Chilotherium* sp.	43	cheek	–8.5	0
M7529	*Chilotherium* sp.	43	cheek	–8.0	5
M7540	*Chilotherium* sp.	43		–7.6	9
M7532	*Chilotherium* sp.	43	cheek	–9.0	0
M7536	*Chilotherium* sp.	43	CHEEK	–9.5	0
M11264	*Gazella* cf. *Gaudryi*	49	rM3	–9.3	0
M11269	*Gazella* cf. *Gaudryi*	49	lm3	–10.6	0
M11270	*Gazella* cf. *Gaudryi*	49	rm3	–11.8	0
M11271	*Gazella* cf. *Gaudryi*	49	rM3	–10.4	0
M11275	*Gazella* cf. *Gaudryi*	49	lm3	–10.7	0
M11322	*Gazella* sp. *paotehensis*	49	rm3	–12.7	0
M11327	*Gazella* sp. *paotehensis*	49	lM3?	–11.9	0
M11328	*Gazella* sp. *paotehensis*	49	lM3	–9.0	0
M11331	*Gazella* sp. *paotehensis*	49	lm3	–10.5	0
M11473	*Gazella* cf. *Dorcadoides*	49	rM3	–8.7	0
M11480	*Gazella* cf. *Dorcadoides*	49	rM1	–7.5	9
M11809	*Tragoreas lagrelii*	49	CHEEK	–11.5	0
M11820	*Tragoreas anderssoni*	49	cheek	–10.3	0

continued

Table 4. Continued.

Sample ID	Taxon	Locality	Tooth	δ^{13}C (PDB)	%C4
M10543	*Urmiatherium intermedium*	49	rp4	–7.5	9
M10546	*Urmiatherium intermedium*	49	rM3	–5.4	27
M10554	*Urmiatherium intermedium*	49		–6.9	14
M10555	*Urmiatherium intermedium*	49	lM3	–9.8	0
M10556	*Urmiatherium intermedium*	49	lM3	–8.6	0
M10557	*Urmiatherium intermedium*	49		–7.7	8
M10573	*Urmiatherium intermedium*	49	lM1	–9.3	0
M10676	*Urmiatherium intermedium*	49	lM3	–7.1	12
M9136	*Cervavitus novorossiae*	49	lm3	–9.6	0
M9143	*Cervavitus novorossiae*	49	lM3	–10.0	0
M9144	*Cervavitus novorossiae*	49	rM2	–9.6	0
M9145	*Cervavitus novorossiae*	49	rM1	–8.9	0
M9146	*Cervavitus novorossiae*	49	rm2	–11.2	0
M992	Pliocervid	49	lm3	–10.9	0
M993	Pliocervid	49	lm3	–9.1	0
M9790	Pliocervid	49	rM3	–9.8	0
M9791	Pliocervid	49	lM3	–9.8	0
M9798	Pliocervid	49	lM3	–9.7	0
M9799	Pliocervid	49	rM3	–10.2	0
M9802	Pliocervid	49	lM3	–10.7	0
M256	*Hipparion hippidiodus*	49	cheek	–7.4	10
M263	*Hipparion plocodus*	49	ldP2	–6.7	16
M3824	*Hipparion platyodus*	49	lp2	–8.8	0
M1741	*Honanotherium schlosseri*	49	M2	–10.7	0
M1742	*Honanotherium schlosseri*	49	lP3	–10.8	0
M1743	*Honanotherium schlosseri*	49	M2	–10.6	0
M1745	*Honanotherium schlosseri*	49	lM3	–9.8	0
M11031	*Paleotragus microdon*	49	lm3	–10.2	0
M11032	*Paleotragus microdon*	49	lM2?	–9.8	0
M11034	*Paleotragus microdon*	49	rm2	–9.7	0
M11036	*Paleotragus microdon*	49	rm1	–11.6	0
M11037	*Paleotragus microdon*	49	rM2	–11.0	0
M10263	*Chleuastochoerus stehlini*	49	rm3	–9.5	0
M10265	*Chleuastochoerus stehlini*	49	m3	–10.5	0
M10267	*Chleuastochoerus stehlini*	49	rm3	–11.6	0
M10268	*Chleuastochoerus stehlini*	49	rm3	–11.6	0
M10270	*Chleuastochoerus stehlini*	49	lm3	–10.7	0
M11185	*Gazella* cf. *gaudryi*	73	lM3	–10.0	0
M11189	*Gazella* cf. *gaudryi*	73	rM3	–11.1	0
M11196	*Gazella* cf. *gaudryi*	73	rm2	–11.8	0
M11197	*Gazella* cf. *gaudryi*	73	rm3	–10.4	0
M11202	*Gazella* cf. *gaudryi*	73	rM3	–10.1	0
M9444	*Cervavitus novorossiae*	73	rM3	–10.2	0
M9445	*Cervavitus novorossiae*	73	lM3	–8.9	0
M9452	*Cervavitus novorossiae*	73	lM3	–9.5	0
M9455	*Cervavitus novorossiae*	73	lM3	–9.8	0
M9457	*Cervavitus novorossiae*	73	rM3	–9.4	0
M350	*Hipparion ptychodus*	73	rP2	–7.8	0
M352	*Hipparion ptychodus*	73	CHEEK	–10.9	0
M354	*Hipparion ptychodus*	73		–10.8	0
M10304	*Chleuastochoerus stehlini*	73	lm2	–10.2	0
M10305	*Chleuastochoerus stehlini*	73	lm2	–11.6	0
M10306	*Chleuastochoerus stehlini*	73	lm2	–11.7	0
M10307	*Chleuastochoerus stehlini*	73	lm3	–11.0	0
M10309	*Chleuastochoerus stehlini*	73	lm3	–10.9	0

continued

Table 4. Continued.

Sample ID	Taxon	Locality	Tooth	δ^{13}C (PDB)	%C4
M11292	*Gazella* sp. *paotehensis*	108	rm3	–9.0	0
M11293	*Gazella* sp. *paotehensis*	108	lm3	–5.7	24
M11294	*Gazella* sp. *paotehensis*	108	rm3	–10.3	0
M11321	*Gazella* sp. *paotehensis*	108	lM3	–8.4	1
M11796	*Tragoreas lagrelii*	108	lm3	–9.5	0
M10530	*Urmiatherium intermedium*	108	lm1	–9.5	0
M10540	*Urmiatherium intermedium*	108	rm2	–7.2	12
M10541	*Urmiatherium intermedium*	108	rm3	–8.3	2
M10686	*Urmiatherium intermedium*	108	lM3	–7.3	11
M355	*Hipparion ptychodus*	108	lp2	–8.5	1
M10987	*Paleotragus microdon*	108	lm3	–9.1	0
M10988	*Paleotragus microdon*	108	lM3	–9.2	0
M10997	*Paleotragus microdon*	108	rM3	–8.4	1
M10998	*Paleotragus microdon*	108	lm3	–11.2	0
M10995	*Paleotragus microdon*	108	lM3	–8.7	0
M7642	*Chilotherium* sp.	108	lM2	–10.1	0
M11309	*Gazella* sp. *paotehensis*	109	lM3	–9.3	0
M11335	*Gazella* sp. *paotehensis*	109	rm3	–9.4	0
M11460	*Gazella* cf. *Dorcadoides*	109	lM2	–8.8	0
M11462	*Gazella* cf. *Dorcadoides*	109	rM3	–7.8	7
M11468	*Gazella* cf. *Dorcadoides*	109	rM3	–8.4	2
M11524	*Gazella* cf. *Dorcadoides*	109	lM3	–9.2	0
M11526	*Gazella* cf. *Dorcadoides*	109	lM3	–7.9	6
M11824	*Tragoreas anderssoni*	109	rm3	–9.2	0
M9711	*Cervavitus novorossiae*	109	rm3	–10.6	0
M9713	*Cervavitus novorossiae*	109	rM3	–10.7	0
M9714	*Cervavitus novorossiae*	109	lM2	–10.1	0
M9716	*Cervavitus novorossiae*	109	lm2	–10.6	0
M11314	*Gazella* sp. *paotehensis*	114	rm3	–8.8	0
M11317	*Gazella* sp. *paotehensis*	114	rm3	–9.8	0
M11319	*Gazella* sp. *paotehensis*	114	lm3	–8.4	2
M11333	*Gazella* sp. *paotehensis*	114	lM3	–9.3	0
M11342	*Gazella* sp. *paotehensis*	114	lM3	–9.5	0
M10405	*Plesiaddax depereti*	114	lm3	–5.8	23
M10406	*Plesiaddax depereti*	114	lm3	–6.4	18
M10407	*Plesiaddax depereti*	114	lm3	–6.3	19
M10408	*Plesiaddax depereti*	114	lm3	–7.0	14
M10486	*Plesiaddax depereti*	114	rM3	–6.3	19
M10487	*Plesiaddax depereti*	114	lM3	–6.8	15
M10485	*Plesiaddax depereti*	114	rM3	–7.9	5
M329	*Hipparion kreugeri*	114	cheek	–8.2	3
M7667	*Chilotherium* sp.	114	dlp3	–6.2	21
M7668	*Chilotherium* sp.	114	lp3	–8.6	0
M7669	*Chilotherium* sp.	114	rp2	–8.5	1
M7667–lM	*Chilotherium* sp.	114	lp3	–8.0	5
M317	*Hipparion kreugeri*	116	lp2	–8.3	2
M318	*Hipparion kreugeri*	116	rp4	–10.9	0
M331	*Hipparion kreugeri*	116	lp2	–8.5	1
M332	*Hipparion kreugeri*	116	CHEEK	–8.8	0
BD.251.YJG03	*Hipparion*	YJG03	m1 or m2	–8.4	2
BD.253.YJG03	*Hipparion*	YJG03	r cheek	–7.3	11
BD.254.YJG03	*Hipparion*	YJG03	cheek	–8.6	0
BD.255.YJG03	*Hipparion*	YJG03	i	–6.9	14
BD.256.YJG03	*Hipparion*	YJG03	r CHEEK	–8.5	0
BD.257.YJG03	*Hipparion*	YJG03	i	–7.5	9

continued

Table 4. Continued.

Sample ID	Taxon	Locality	Tooth	δ^{13}C (PDB)	%C4
BD.259.YJG03	*Hipparion*	YJG03	lP2	–8.8	0
BD.262.YJG03	*Hipparion*	YJG03	rP4	–7.5	9
BD.265.YJG03	*Hipparion*	YJG03	rM1	–8.1	4
BD.266.YJG03	*Hipparion*	YJG03	lm3	–9.1	0
BD.268.YJG03	*Hipparion*	YJG03	rP4	–7.9	6
BD.269.YJG03	*Hipparion*	YJG03	rM3	–9.3	0
BD.270.YJG03	*Hipparion*	YJG03	r cheek	–8.2	3
BD.271.YJG03	*Hipparion*	YJG03	r cheek	–7.7	7
BD.273.YJG03	*Hipparion*	YJG03	CHEEK	–9.0	0
BD.274.YJG03	*Hipparion*	YJG03	lP	–8.4	2
BD.275.YJG03	*Hipparion*	YJG03	cheek	–6.9	14
BD.277.YJG03	*Hipparion*	YJG03	lP3	–8.0	5
BD.280.YJG03	*Hipparion*	YJG03	rm1	–8.8	0
BD.281.YJG03	*Hipparion*	YJG03	lM2	–8.7	0
BD.250.YJG03	*Samotherium*	YJG03	lm3	–7.3	11
BD.260.YJG03	*Samotherium*	YJG03	P	–7.3	11
BD.261.YJG03	*Samotherium*	YJG03	P	–7.4	10
BD.263.YJG03	*Samotherium*	YJG03	rdP4	–8.1	4
BD.264.YJG03	*Samotherium*	YJG03	P	–7.4	10
BD.272.YJG03	*Samotherium*	YJG03	lM	–7.6	9
BD.278.YJG03	*Samotherium*	YJG03	P	–6.8	15

locality 30: *G. paotehense* had a pure C3 diet, while *G. dorcadoides* had a component of C4. In contrast, at the older locality 49, gazelles showed consistent browser diet with pure C3 signal, with the exception of one *G. dorcadoides* individual showing a minor (< 10%) C4 component in its diet. Similar to gazelles, the hipparion mesowear results were also consistent with isotope results: Isotope data from locality 108 and mesowear results from locality 44 suggested browsing with C3 dominated diet, while localities 49 and 43 showed more mixed isotope signal. On the other hand, hipparions at locality 30 showed much more clearly grazer-dominated diet according to mesowear results, while isotope results varied more.

Chilotherium data were interesting: the mesowear signal suggested that it was a grazer at locality 43, but then changed to browsing at locality 30. Isotope values from these localities overlap, so they are hard to interpret. With *Urmiatherium* the situation was similar to hipparions: the intermediate locality 108 shows a more browser-dominated/C3 dominated signal than localities 49 or 43, while locality 30 was clearly grazer-dominated with a C4 component.

Samotherium at locality 30 had a high C4 component and groups with grazers (by mesowear), but isotopically there was no change between older (YJG-03) and younger (locality 30) localities. *Paleotragus* mesowear was quite consistent with isotopes: it was a mixed feeder or browser at older localities (49 and 108) with a pure C3 diet, and at locality 30 it was a grazer with a C4 component. *Tragoreas* isotopes showed that at localities 108 and 49 their diet was more browse dominated than at localities 43 or 30.

Discussion and conclusions

According to our results, it seems that the youngest locality 30 had a much harsher (more arid conditions with more abrasive food resources for herbivores) environment than the rest of the localities, confirming earlier results (Liu *et al.* 2008, Kaakinen *et al.* 2013). Our precipitation estimates suggested that the oldest locality 49 differed considerably from other old and intermediate localities, due to its more humid conditions. In contrast, locality 30 had much less precipitation than any other locality analysed here. Since precipitation in this region is primar-

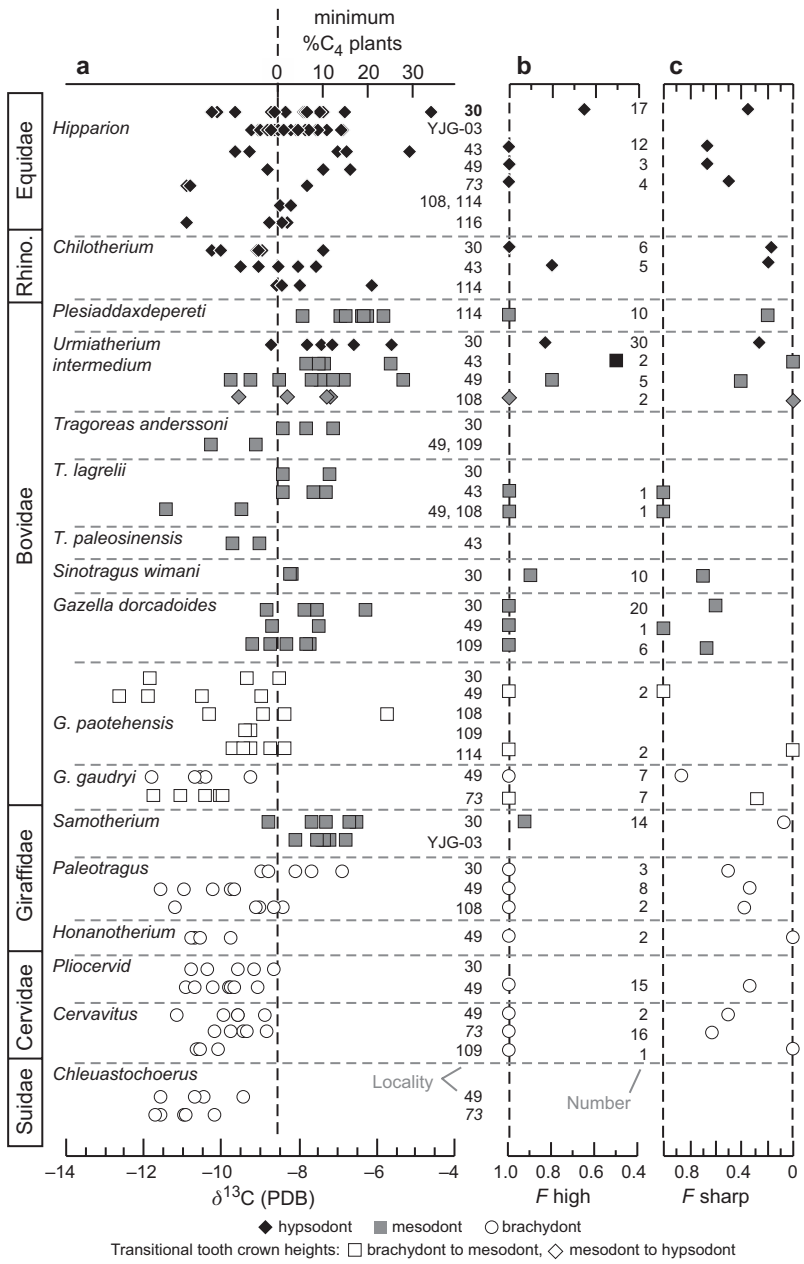

Fig. 3. Carbon isotope and mesowear data for Baodean herbivores. Numbers in boldface indicate "dorcadoides" localities, in regular face mixed localities, and in italics "gaudryi" localities. In **b**, mesowear cusp relief is indicated by the fraction of specimens exhibiting high relief; this completely describes cusp relief because cusps can only be high or low. In **c**, mesowear cusp shape is described by the fraction of individuals with sharp cusps. Because very few individuals have blunt cusps, this plot describes cusp shape mainly as sharp versus round. 'Number' refers to the number of individuals examined for mesowear.

ily governed by the East Asian summer monsoon strength, the difference in the estimated precipitation between the old (e.g., 49) and young (e.g., 30) localities implies a significant decrease in the East Asian summer monsoon strength during 7–5.7 Ma in the Baode region. The many monsoon proxy records used to interpret East Asian summer monsoon changes over 7–5 Ma offer contradictory conclusions. While some evidence suggests a general strengthening trend of the East Asian summer monsoon during 7–5 Ma (e.g., Ding *et al*. 1999, An *et al*. 2001, Jia *et al*. 2003, Sun *et al*. 2010), other evidence points to a declining East Asian summer monsoon (Ma *et al*. 1998, Wan *et al*. 2006) or no change during this period (Jiang & Ding 2008). Our results suggested a weakening of the East Asian summer monsoon in the Baode region, which may have resulted from global cooling and the emergence of the northern hemispheric ice sheet (Passey *et*

al. 2009). In addition, a recent climate model study implicates growth of the Zagros Mountains possibly contributing to the decline of the East Asian summer monsoon, therefore leading to the decrease of precipitation over the Baode region (Tang *et al*. 2013).

Our synthesized data also shed light on the dynamics of the change from the more mesic conditions (represented by the oldest locality 49) to the harsh conditions (represented by the youngest locality 30) in the Baode region. Although the intermediate localities (44 and 108) had more browse-dominated faunas than the older localities in our analyses, they seemed to show highly variable conditions in both dietary adaptations (as shown by mesowear and isotopes) as well as environmental conditions (as shown by hypsodonty precipitation proxy estimates) as compared with the oldest and youngest localities. As all of the studied localities were situated within a few kilometres of each other, the differences in topography and sedimentary environment for fossil preservation were small (*see* the discussion above in the description of the study area), and therefore cannot explain the more variable conditions in the intermediate localities. As the Baode region is situated in the middle of the monsoon transition zone (*see* Passey *et al*. 2009), we argue that the more variable conditions manifested in the fossil records of the intermediate localities might reflect the nature of the transitional climate from humid (strong monsoon) to dry (weak monsoon) conditions. For instance, vegetation in this transition period might be more mosaic. Patches of C3 forest and C4 grass coexisted on the landscape, and thus were recorded by mammal species with different diet preferences. It is equally possible that, during the transition period, monsoon climate in Baode might exhibited larger temporal variability on different time scales, which were recorded by our fossil records. Climate model studies on the Asian monsoon climate have mostly focused on the early Late Miocene (11–7 Ma) (Micheels *et al*. 2011, Tang *et al*. 2011) and the mid-Pliocene (around 4 Ma) (Zhang *et al*. 2013a). However, there are few climate model studies on the Asian monsoon climate changes at 7–5 Ma (i.e., late Late Miocene–Early Pliocene), which could be a future study topic in order to better understand the climate processes underlying the changes shown in our fossil records.

Acknowledgements

We thank Mikael for taking us on a fascinating academic journey — it has been exciting, new, and never dull, and most importantly — fun. We also thank Mikael for his support and guidance through various stages of our careers, and we hope this is just the beginning. Larry Flynn, Pirkko Ukkonen and Suvi Viranta-Kovanen gave helpful and constructive comments. Additionally, we want to acknowledge all the financial support that the Fenno-American-Chinese work in North China has received during many years. These include: the Strategic Priority Research Program of Chinese Academy of Sciences (XDB03020501) and the national Basic Research Program of China (2012CB821900), Academy of Finland, the Ella & Georg Ehrnrooth Foundation, the Finnish Cultural Foundation, the Emil Aaltonen Foundation, National Geographic Society, and the U.S. National Science Foundation.

References

An, Z. S., Kutzbach, J. E., Prell, W. L. & Porter, S. C. 2001: Evolution of Asian monsoons and phased uplift of the Himalayan Tibetan plateau since Late Miocene times. — *Nature* 411: 62–66.

Anderson, J. G. 1923: Essays on the Cenozoic of northern China. — *Geological Survey of China Memoir, Series A* 3: 1–152.

Ding, Z. L., Xiong, S. F., Sun, J. M., Yang, S. L., Gu, Z. Y. & Liu, T. S. 1999: Pedostratigraphy and paleomagnetism of a 7.0 Ma eolian loess-red clay sequence at Lingtai, Loess Plateau, north-central China and the implications for paleomonsoon evolution. — *Palaeogeography Palaeoclimatology Palaeoecology* 152: 49–66.

Eronen, J. T., Puolamäki, K., Liu, L., Lintulaakso, K., Damuth, J., Janis, C. & Fortelius, M. 2010: Precipitation and large herbivorous mammals, part I: Estimates from present-day communities. — *Evolutionary Ecology Research* 12: 217–233.

Fortelius, M. & Solounias, N. 2000: Functional characterization of ungulate molars using the abrasion-attrition wear gradient: a new method for reconstructing paleodiets. — *American Museum Novitates* 3301: 1–36.

Fortelius, M., Eronen, J. T., Jernvall, J., Liu, L. P., Pushkina, D., Rinne, J., Tesakov, A., Vislobokova, I., Zhang, Z. Q. & Zhou, L. P. 2002: Fossil mammals resolve regional patterns of Eurasian climate change over 20 million years. — *Evolutionary Ecology Research* 4: 1005–1016.

Guo, Z. T., Ruddiman, W. F., Hao, Q. Z., Wu, H. B., Qiao, Y. S., Zhu, R. X., Peng, S. Z., Wei, J. J., Yuan, B. Y. & Liu, T. S. 2002: Onset of Asian desertification by 22 Myr ago inferred from loess deposits in China. — *Nature* 416: 159–163.

Jia, G. D., Peng, P. A., Zhao, Q. H. & Jian, Z. M. 2003: Changes in terrestrial ecosystem since 30 Ma in East Asia: stable isotope evidence from black carbon in the South China Sea. — *Geology* 31: 1093–1096.

Jiang, H. C. & Ding, Z. L. 2008: A 20 Ma pollen record of East-Asian summer monsoon evolution from Guyuan, Ningxia, China. — *Palaeogeography Palaeoclimatology Palaeoecology* 265: 30–38

Kaakinen, A. & Lunkka, J. P. 2003: Sedimentation of the Late Miocene Bahe Formation and its implications for stable environments adjacent to Qinling Mountains in Shaanxi, China. — *Journal of Asian Earth Sciences* 22: 67–78.

Kaakinen, A. 2005: *A long terrestrial sequence in Lantian – a window into the late Neogene palaeoenviornments of northern China*. — Ph.D. thesis, Department of Geology, University of Helsinki.

Kaakinen, A., Passey, B. H., Zhang, Z., Liu, L., Pesonen, L. J. & Fortelius, M. 2013: Stratigraphy and paleoecology of the classical dragon bone localities of Baode County, Shanxi Province. — In: Wang, X. M., Fortelius, M. & Flynn, L. (eds.), *Fossil mammals of Asia: Neogene biostratigraphy and chronology*: 203–217. Columbia University Press, New York.

Kurtén, B. 1952: The Chinese Hipparion fauna. — *Commentationes Biological, Societas Scientiarum Fennica* 13: 1–82.

Kurtén, B. 1953: On the variation and population dynamics of fossil and recent mammal populations. — *Acta Zoologica Fennica* 76: 1–122.

Kurtén, B. 1985: *Thalassictus wongii* (Mammalia, Hyaenidae) and related forms from China and Europe. — *Bulletin of the Geological Institutions of the University of Uppsala* 11: 79–90.

Li, C., Wu, W. & Qiu, Z. 1984: Chinese Neogene: Subdivision and correlation. — *Vertebrata PalAsiatica* 22: 163–178. [In Chinese with English summary].

Liu, D., Li, C. & Zhai, R. 1978: [Pliocene vertebrates from Lantian, Shensi: Tertiary mammalian fauna of the Lantian District, Shensi]. *Professional Papers of Stratigraphy and Paleontology* 7: 149–200. [In Chinese].

Liu, L., Zhang, Z., Cui, N. & Fortelius, M. 2008: The Dipodidae (Jerboas) from Loc.30 and their environmental significance. — *Vertebrata PalAsiatica* 46: 125–132.

Liu, L., Puolamäki, K. Eronen, J. T., Mirzaie, M., Hernesniemi, E. & Fortelius, M. 2012: Estimating net primary productivity from dental traits. — *Proceedings of the Royal Society B* 279: 2793–2799.

Lu, H., Vandenberghe, J. & An, Z. 2001: Aeolian origin and palaeoclimatic implications of the 'Red Clay' (north China) as evidenced by grain-size distribution. — *Journal of Quaternary Science* 16: 89–97.

Ma, Y. Z., Li, J. J. & Fang, X. M. 1998: Pollen assemblage in 30.6–5.0 Ma redbeds of Linxia region and climate evolution. — *Chinese Science Bulletin* 43: 301–304.

Micheels, A., Bruch, A. A., Eronen, J. T., Fortelius, M., Harzhauser, M., Utescher, T. & Mosbrugger, V. 2011: Analysis of heat transport mechanisms from a Late Miocene model experiment with a fully-coupled atmosphere-ocean general circulation model. — *Palaeogeography Palaeoclimatology Palaeoecology* 304: 337–350.

Pan, B., Hu, Z., Wang, J., Vandenberghe, J. & Hu, X. 2011: A magnetostratigraphic record of landscape development in the eastern Ordos Plateau, China: Transition from the Late Miocene and Early Pliocene stacked sedimentation to the Late Pliocene and Quaternary uplift and incision by the Yellow River. — *Geomorphology* 125: 225–238.

Passey, B. H. 2007: *Stable isotope paleoecology: Methodological advances and applications to the late Neogene environmental history of China*. — Ph.D. thesis, University of Utah.

Passey, B. H., Eronen, J. T., Fortelius, M. & Zhang, Z. Q. 2007: Paleodiets and paleoenvironments of late Miocene gazelles from North China: Evidence from stable carbon isotopes. — *Vertebrata PalAsiatica* 45: 118–127.

Passey, B. H., Ayliffe, L. K., Kaakinen, A., Zhang, Z., Eronen, J. T., Zhu, Y., Zhou, L., Cerling, T. E. & Fortelius, M. 2009: Strengthened East Asian summer monsoons during a period of high-latitude warmth? Isotopic evidence from Mio-Pliocene fossil mammals and soil carbonates from northern China. — *Earth and Planetary Science Letters* 277: 443–452.

Qiu, Z. & Qiu, Z. 1995: Chronological sequence and subdivision of Chinese Neogene mammalian faunas. — *Palaeogeography Palaeoclimatology Palaeoecology* 166: 41–70.

Schlosser, M. 1903: Die fossilen Säugethiere Chinas nebst einer Odontographie der recenten Antilopen. — *Abhandlungen der Bayerischen Akademie der Wissenschaften* 22: 1–221.

Sukselainen, L. 2008: *The Late Miocene climate in northern Loess Plateau as recorded by magnetic susceptibility and grain size of the Red Clay from Baode, Shanxi Province, China*. — M.Sc. thesis, University of Helsinki.

Sun, Y., An, Z., Clemens, S. C., Bloemendal, J. & Vandenberghe, J. 2010: Seven million years of wind and precipitation variability on the Chinese Loess Plateau. — *Earth and Planetary Science Letters* 297: 525–535.

Tang, H. 2013: *The spatio-temporal evolution of the Asian monsoon climate in the Late Miocene and its causes: A regional climate model study*. — Ph.D. thesis, University of Helsinki.

Tang, H., Micheels, A., Eronen, J. T. & Fortelius, M. 2011: Regional climate model experiments to investigate the Asian monsoon in the Late Miocene. — *Climate of the Past* 7: 847–868.

Tang, H., Micheels, A., Eronen, J. T., Ahrens, B. & Fortelius, M. 2013: Asynchronous responses of East Asian and Indian summer monsoons to mountain uplift shown by regional climate modelling experiments. — *Climate Dynamics* 40: 1531–1549.

Wan, S. M., Li, A. C., Clift, P. D. & Jiang, H. Y. 2006: Development of the East Asian summer monsoon: Evidence from the sediment record in the South China Sea since 8.5 Ma. — *Palaeogeography Palaeoclimatology Palaeoecology* 241: 139–159.

Zdansky, O. 1923: Fundorte der Hipparion-Fauna um Pao-Te-Hsien in NW-Shansi. — *Bulletin of the Geological Survey of China* 5: 69–81.

Zhang, R., Yan, Q., Zhang, Z. S., Jiang, D., Otto-Bliesner, B.

L., Haywood, A. M., Hill, D. J., Dolan, A. M., Stepanek, C., Lohmann, G., Contoux, C., Bragg, F., Chan, W.-L., Chandler, M. A., Jost, A., Kamae, Y., Abe-Ouchi, A., Ramstein, G., Rosenbloom, N. A., Sohl, L. & Ueda, H. 2013a: East Asian monsoon climate simulated in the PlioMIP. — *Climate of the Past* 9: 2085–2099.

Zhang, Z., Kaakinen, A., Liu L., Lunkka, J. P., Sen, S., Qiu Z., Zheng, S. & Fortelius, M. 2013b: Mammalian Biochronology of the Late Miocene Bahe Formation. — In: Wang, X. M., Fortelius, M. & Flynn, L. (eds.), *Fossil mammals of Asia: Neogene biostratigraphy and chronology*: 187–202. Columbia University Press, New York.

Zhang, Z., Gentry, A., Kaakinen, A., Liu, L., Lunkka, J. P., Qiu, Z., Sen, S., Scott, R. S., Werdelin, L., Zheng, S. & Fortelius, M. 2002: Land mammal faunal sequence of the late Miocene of China: new evidence from Lantian, Shaanxi Province. — *Vertebrata PalAsiatica* 40: 165–176.

Zhu, Y., Zhou, L., Mo, D., Kaakinen, A., Zhang, Z. & Fortelius, M. 2008: A new magnetostratigraphic framework for late Neogene Hipparion Red Clay in the eastern Loess Plateau of China. — *Palaeogeography Palaeoclimatology Palaeoecology* 268: 47–57.